Variations in the optical scattering properties of phytoplankton cultures

Wen Zhou,[1,*] Guifen Wang, [1] Zhaohua Sun, [1] Wenxi Cao,[1] Zhantang Xu,[1] Shuibo Hu,[1,2] and Jun Zhao[3]

[1]*State Key Laboratory of Tropical Oceanography, South China Sea Institute of Oceanology, Chinese Academy of Sciences, Guangzhou 510301, China*
[2]*Graduate School of Chinese Academy of Science, Beijing,100039, China*
[3]*College of Marine Science, University of South Florida, 140 Seventh Avenue, South, Saint Petersburg, Florida 33701, USA*
[*]*wenzhou@scsio.ac.cn*

Abstract: The scattering and backscattering coefficients of 15 phytoplankton species were determined in the laboratory using the acs and BB9 instruments. The spectral variability of scattering properties was investigated and the homogenous sphere model based on Mie theory was also evaluated. The scattering efficiencies at 510 nm varied from 1.42 to 2.26, and the backscattering efficiencies varied from 0.003 to 0.020. The backscattering ratios at 510 nm varied from 0.17% to 0.97%, with a mean value of 0.58%. The scattering properties were influenced by algal cell size and cellular particulate organic carbon content rather than the chlorophyll a concentration. Comparison of the measured results to the values estimated using the homogenous sphere model showed that: (1) The model could well reproduce the spectral scattering coefficient with relative deviations of 5–39%, which indicates that cell shape and internal structure have no significant effects on predicting the scattering spectra; (2) Although the homogenous sphere model generally reflected the spectral trend of backscattering spectra for most species, it severely underestimated the backscattering coefficients by 1.4–48.6 folds at 510 nm. The deviations for *Chaetoceros* sp. and *Microcystis aeruginosa* were large and might be due to algal cell chain links and intracellular gas vacuoles, respectively.

OCIS codes: (010.4450) Oceanic optics; (010.1350) Backscattering; (290.5850) Scattering, particles.

References and links

1. C. S. Roesler and S. L. McLeroy-Etheridge, "Remote detection of harmful algal blooms," in *Ocean Optics XIV*, S. G. Ackleson and R. Frouin, eds. (SPIE, 1998), pp. 117–128.
2. J. P. Cannizzaro, K. L. Carder, F. R. Chen, C. A. Heil, and G. A. Vargo, "A novel technique for detection of the toxic dinoflagellate, *Karenia brevis*, in the Gulf of Mexico from remotely sensed ocean color data," Cont. Shelf Res. **28**(1), 137–158 (2008).
3. T. S. Kostadinov, D. A. Siegel, and S. Maritorena, "Retrieval of the particle size distribution from satellite ocean color observations," J. Geophys. Res. **114**(C9), C09015 (2009).
4. T. S. Kostadinov, D. A. Siegel, and S. Maritorena, "Global variability of phytoplankton functional types from space: assessment via the particle size distribution," Biogeosciences Discuss. **7**(3), 4295–4340 (2010).
5. A. Bricaud and A. Morel, "Light attenuation and scattering by phytoplanktonic cells: a theoretical modeling," Appl. Opt. **25**(4), 571–580 (1986).
6. D. Stramski, A. Morel, and A. Bricaud, "Modeling the light attenuation and scattering by spherical phytoplanktonic cells: a retrieval of the bulk refractive index," Appl. Opt. **27**(19), 3954–3956 (1988).
7. S. Bernard, T. A. Probyn, and R. G. Barlow, "Measured and modeled optical properties of particulate matter in the southern Benguela," S. Afr. J. Sci. **97**, 410–420 (2001).
8. A. Bricaud, A. L. Bedhomme, and A. Morel, "Optical properties of diverse phytoplanktonic species: experimental results and theoretical interpretation," J. Plankton Res. **10**(5), 851–873 (1988).
9. Y. H. Ahn, A. Bricaud, and A. Morel, "Light backscattering efficiency and related properties of some phytoplankters," Deep-Sea Res. **39**(11-12), 1835–1855 (1992).

#161249 - $15.00 USD Received 11 Jan 2012; revised 18 Apr 2012; accepted 19 Apr 2012; published 1 May 2012

10. D. Stramski and R. A. Reynolds, “Diel variations in the optical properties of a marine diatom,” Limnol. Oceanogr. **38**(7), 1347–1364 (1993).
11. D. Stramski, G. Rosenberg, and L. Legendre, “Photosynthetic and optical properties of the marine chlorophyte *Dunaliella tertiolecta* grown under fluctuating light caused by surface wave focusing,” Mar. Biol. **115**(3), 363–372 (1993).
12. D. Stramski, A. Sciandra, and H. Claustre, “Effects of temperature, nitrogen, and light limitation on the optical properties of the marine diatom *Thalassiosira pseudonana*,” Limnol. Oceanogr. **47**(2), 392–403 (2002).
13. D. Stramski, A. Bricaud, and A. Morel, “Modeling the inherent optical properties of the ocean based on the detailed composition of the planktonic community,” Appl. Opt. **40**(18), 2929–2945 (2001).
14. D. Stramski, E. Boss, D. Bogucki, and K. J. Voss, “The role of seawater constituents in light backscattering in the ocean,” Prog. Oceanogr. **61**(1), 27–56 (2004).
15. J. C. Kitchen and J. R. V. Zaneveld, “A three-layered sphere model of the optical properties of phytoplankton,” Limnol. Oceanogr. **37**(8), 1680–1690 (1992).
16. A. Bricaud, J. R. V. Zaneveld, and J. C. Kitchen, “Backscattering efficiency of cocoolithophorids: use of a three-layered sphere model,” Proc. SPIE **1750**, 27–33 (1992).
17. A. Quirantes and S. Bernard, “Light scattering by marine algae: two-layer spherical and nonspherical models,” J. Quant. Spectrosc. Radiat. Transf. **89**(1-4), 311–321 (2004).
18. W. R. Clavano, E. Boss, and L. Karp-Boss, “Inherent optical properties of non-spherical marine like particles—from theory to observation,” in *Oceanography and Marine Biology: an Annual Review*, R. N. Gibson, R. J. A. Atkinson, and J. D. M. Gordon, eds. (Taylor & Francis, 2007), Vol. 45, pp. 1–38.
19. A. Quirantes and S. Bernard, “Light scattering methods for modeling algal particles as a collection of coated and/or nonspherical scatterers,” J. Quant. Spectrosc. Radiat. Transf. **100**(1-3), 315–324 (2006).
20. M. S. Quinby-Hunt, A. J. Hunt, K. Lofftus, and D. Shapiro, “Polarized-light scattering studies of marine Chlorella,” Limnol. Oceanogr. **34**(8), 1587–1600 (1989).
21. H. Volten, J. F. de Haan, J. W. Hovenier, R. Schreurs, W. Vassen, A. G. Dekker, H. J. Hoogenboom, F. Charlton, and R. Wouts, “Laboratory measurements of angular distributions of light scattered by phytoplankton and silt,” Limnol. Oceanogr. **43**(6), 1180–1197 (1998).
22. K. Witkowski, T. Król, A. Zieliński, and E. Kuteń, “A light-scattering matrix for unicellular marine phytoplankton,” Limnol. Oceanogr. **43**(5), 859–869 (1998).
23. R. D. Vaillancourt, C. W. Brown, R. R. L. Guillard, and W. M. Balch, “Light backscattering properties of marine phytoplankton: relationships to cell size chemical composition and taxonomy,” J. Plankton Res. **26**(2), 191–212 (2004).
24. A. L. Whitmire, W. S. Pegau, L. Karp-Boss, E. Boss, and T. J. Cowles, “Spectral backscattering properties of marine phytoplankton cultures,” Opt. Express **18**(14), 15073–15093 (2010).
25. G. Dall’Olmo, T. K. Westberry, M. J. Behrenfeld, E. Boss, and W. H. Slade, “Significant contribution of large particles to optical backscattering in the open ocean,” Biogeosciences **6**(6), 947–967 (2009).
26. J. M. Sullivan, M. S. Twardowski, J. R. V. Zaneveld, C. M. Moore, A. H. Barnard, P. L. Donaghay, and B. Rhoades, “Hyperspectral temperature and salt dependencies of absorption by water and heavy water in the 400-750 nm spectral range,” Appl. Opt. **45**(21), 5294–5309 (2006).
27. R. A. Maffione and D. R. Dana, “Instruments and methods for measuring the backward-scattering coefficient of ocean waters,” Appl. Opt. **36**(24), 6057–6067 (1997).
28. A. Knap, A. Michaels, A. Close, H. Ducklow, and A. Dickson, *Protocols for the Joint Global Ocean Flux Study (JGOFS) Core Measurements*, JGOFS Report No. 19 (Reprint of the IOC Manuals and Guides No. **29**, UNESCO, Paris, 1994).
29. F. Vidussi, H. Claustre, J. Bustillos-Guzman, C. Cailliau, and J. C. Marty, “Determination of chlorophylls and carotenoids of marine phytoplankton: separation of chlorophyll a from divinyl-chlorophyll a and zeaxanthin from lutein,” J. Plankton Res. **18**(12), 2377–2382 (1996).
30. J. R. V. Zaneveld and J. C. Kitchen, ““The scattering error correction of reflecting-tube absorption waters,” Proc. SPIE **2258**, 44–55 (1994).
31. A. Bricaud, A. Morel, and L. Prieur, “Optical efficiency factors of some phytoplankters,” Limnol. Oceanogr. **28**(5), 816–832 (1983).
32. A. Morel and A. Bricaud, “Inherent optical properties of algal cells, including picoplankton. Theoretical and experimental results,” Can. Bull. Fish. Aquat. Sci. **214**, 521–559 (1986).
33. A. Morel, “Optics of marine particles and marine optics,” in *Particle Analysis in Oceanography* S.Demers, ed., NATO ASI Series. G27 (1991) pp. 141–188.
34. A. Morel and A. Bricaud, “Theoretical results concerning light absorption in a discrete medium, and application to specific absorption of phytoplankton,” Deep-Sea Res. **28**(11), 1375–1393 (1981).
35. E. Boss, R. Collier, G. Larson, K. Fennel, and W. S. Pegau, “Measurements of spectral optical properties and their relation to biogeochemical variables and processes in Crater Lake, Crater Lake National Park, OR,” Hydrobiologia **574**(1), 149–159 (2007).
36. D. Stramski, R. A. Reynolds, M. Babin, S. Kaczmarek, M. R. Lewis, R. Röttgers, A. Sciandra, M. Stramska, M. S. Twardowski, B. A. Franz, and H. Claustre, “Relationships between the surface concentration of particulate organic carbon and optical properties in the eastern South Pacific and eastern Atlantic Oceans,” Biogeosciences **5**(1), 171–201 (2008).

#161249 - $15.00 USD Received 11 Jan 2012; revised 18 Apr 2012; accepted 19 Apr 2012; published 1 May 2012

37. D. Stramski, "Refractive index of planktonic cells as a measure of cellular carbon and chlorophyll a content," Deep Sea Res. Part I Oceanogr. Res. Pap. **46**(2), 335–351 (1999).
38. H. J. Hu and Y. X. Wei, *The Freshwater Algal of China, Systematics, Taxonomy and Ecology* (Science Publisher, 2006).
39. E. Aas, "Refractive index of phytoplankton derived from its metabolite composition," J. Plankton Res. **18**(12), 2223–2249 (1996).
40. S. Liu, "Dynamic effects of phosphorus in plankton ecosystem in the Pearl River Estuary and adjacent waters," Ph.D dissertation (Graduate School of Chinese Academy of Science, 2005.
41. H. Guo, *Illustrations of Planktons Responsible for the Blooms in Chinese Coastal Waters* (Oceanpress, 2004).
42. S. Bernard, T. A. Probyn, and A. Quirantes, "Simulating the optical properties of phytoplankton cells using a two-layered spherical geometry," Biogeosciences Discuss. **6**(1), 1497–1563 (2009).
43. D. Stramski and J. Piskozub, "Estimation of scattering error in spectrophotometric measurements of light absorption by aquatic particles from three-dimensional radiative transfer simulations," Appl. Opt. **42**(18), 3634–3646 (2003).
44. J. R. V. Zaneveld and J. C. Kitchen, "The variation in the inherent optical properties of phytoplankton near an absorption peak as determined by various models of cell structure," J. Geophys. Res. **100**(C7), 13309–13320 (1995).

1. Introduction

Light scattering and backscattering coefficients of diverse phytoplankton are key parameters determining the optical variability of oceanic waters and their reflectance properties. Thus, knowledge of these parameters could be extremely useful in the optical detection of dominant phytoplankton species during blooms [1,2] and in the evaluation of phytoplankton community structure in the ocean [3,4]. To date, however, variations in the scattering properties of diverse phytoplankton species remain poorly understood. This is especially true for backscattering properties, which are difficult to measure at sufficient angular and spectral ranges.

Historically, theoretical calculations have been used to interpret the variability of the scattering and backscattering coefficients of phytoplankton. A homogenous sphere model, which is based on the anomalous diffraction approach of van de Hulst, was developed to predict scattering and backscattering coefficients [5–7]. This model was tested on data measured using a spectrophotometer equipped with an integrating sphere [5,8,9]. It has been used in numerous types of optical oceanography studies, including investigation of the variability of the scattering properties of phytoplankton under varying environmental conditions [10–12] and in assessments of the role of the phytoplankton community in light scattering and backscattering in the ocean [13,14]. However, the hypothesis of a homogenous sphere, which is central to this model, is a potential shortcoming when estimating the scattering properties of phytoplankton. In reality, algal cells might possess a variety of complex internal structures and shapes, many of which would significantly deviate from the homogeneous spherical structure. Theoretical calculations for layered particles [15–17] and non-spherical particles [18] indicate that both cell shape and intracellular structure have a significant effect on scattering properties. A limited number of measurements also have shown a potential departure from the homogenous sphere simulation for scattering properties [19], especially for the volume scattering function [20–22].

Recently, commercial instruments (e.g., acs, ac9, BB9 (WET Labs Inc.), or HS6 (HOBI Inc.)) became available for direct estimation of scattering properties. The scattering properties of several algae species have been estimated in the laboratory using commercial ac9 and HS6 meters [23,24]. For example, Vaillancourt et al. [23] observed that the backscattering spectra of 29 species followed the power law function, and plankton backscattering coefficients at 510 nm were well correlated with particulate organic carbon (POC) content rather than chlorophyll a (Chl a) concentration and cell density. They found that the refractive indices derived from inversion of Mie theory to backscattering were generally higher than published values for phytoplankton, which therefore suggested that the Mie theory for homogenous spherical particles could not adequately reproduce the backscattering of phytoplankton. Whitmire et al. [24], who estimated the backscattering coefficients of 13 phytoplankton

#161249 - $15.00 USD Received 11 Jan 2012; revised 18 Apr 2012; accepted 19 Apr 2012; published 1 May 2012

species, observed large intra- and interspecific variability in the backscattering spectra. They established a relationship between cell size and both the backscattering ratio and backscattering cross-section. They also found that their observed backscattering cross-section was up to one order of magnitude higher than that the modeled values from Stramski et al. [13]. Thus, they suggested that Mie theory was likely to underestimate backscattering for non-spherical and inhomogeneous particles. Other work in the field also suggests that backscattering from phytoplankton is underestimated using the Mie theory for homogenous sphere [25].

Currently, many questions remain about the spectral variability of phytoplankton backscattering and the inappropriateness of theoretical models. For example, it is unclear how phytoplankton characteristics such as size, shape, and internal structure affect their backscattering properties. Some studies have reported that Mie theory for homogenous spheres underestimates the magnitude of spectral backscattering properties of phytoplankton cells [23,24]. However, spectral backscattering measurements of phytoplankton cultures determined using commercial backscattering instruments are rare in the literature. Furthermore, few studies have reported quantitative results of comparisons between the spectral backscattering properties estimated using instruments and those spectra predicted by the homogenous sphere model.

In this study, we estimated the spectral scattering and backscattering coefficients of 15 phytoplankton species from 6 taxa in the laboratory using acs and BB9 meters. We also measured algal cell size, POC content, and Chl a concentration. The objective of this study was to investigate the spectral variability of the scattering properties of algal cultures and to identify the factors that influence these scattering properties. We also quantitatively compared the measurements with the results predicted by the homogenous sphere model in order to rigorously assess the appropriateness of using this model for algal species with diverse cell morphology and intracellular structure.

2. Methods

2.1 Phytoplankton cultures

Cultures representing 15 species from 6 major taxa (Table 1) were supplied by the Marine Biology Group of the South China Sea Institute of Oceanography. All cultures were grown in f2-enriched medium that was sterilized and filtered using 0.45 μm filter membranes. The cultures were incubated at 20 ± 1 °C under a 12:12 dark: light cycle. The algal cell density was counted by light microscopy every day to identify the exponential growth stage for all species. These cultures were not axenic. The bacterial contamination accounted for about 2–5% of the algal cell density in most cultures. Many of the bacteria were about 0.2 μm in size.

2.2 Optical measurements

All measurements were completed during the exponential growth stage of the cultures. The spectral absorption and attenuation coefficients were measured using an acs meter (WET Labs Inc.). The volume scattering functions at 117° were measured using a BB9 meter, and measurements were then converted to estimate the backscattering coefficients.

BB9 measurements were performed in a $320 \times 320 \times 400$ mm^3 (length, width, and height, respectively) plexiglass box wrapped with an opaque black cloth.

The BB9 meter was suspended above the container so that the divergence lights emitted from the light sources of the BB9 instrument were completely directed into the bottom of the container. We rotated the BB9 in the container and collected measurements in several orientations; none of the data were significantly different among these varying orientations. However, the same instrument orientation was used in each experiment to eliminate any possible deviation. The acs measurements were conducted by circulating the sample medium from the box through tubing to the acs and then back into the box. The measurements were

#161249 - $15.00 USD Received 11 Jan 2012; revised 18 Apr 2012; accepted 19 Apr 2012; published 1 May 2012

Table 1. Summary of Phytoplankton Characteristics

Name	Class	Shape	ESD (μm)	Chl a (pg cell^{-1})	Carbon (pg cell^{-1})
Prymnesium patelliferum	Haptophyceae	oval	7.9	0.76	54.8
Phaeocystis sp.	Haptophyceae	sphere	4.0	0.05	18.5
Amphidinium sp.	Dinophyceae	bioconical	5.0	0.31	14.0
Chattonella marina	Raphidophyceae	oval	12.1	4.52	197.0
Microcystis aeruginosa	Cyanophyceae	oval	4.5	0.10	14.2
Nitzschia closterium	Diatomacae	fasiform	4.4	–	17.8
Thalassirosira weissflogii	Diatomacae	cylinder	12.8	1.62	–
Thalassirosira pseudonana	Diatomacae	cylinder	4.8	0.15	–
Biddulphiales sp.	Diatomacae	short-box	7.0	0.74	42.3
Chaetoceros sp.	Diatomacae	ell-cylinder	6.5	0.17	35.2
Dunaliella tertiolecta	Chlorophyceae	oval	10.2	2.56	102.7
Tetraselmis levis	Chlorophyceae	oval	12.0	–	–
Chlorella sp.	Chlorophyceae	sphere	6.0	0.33	52.7
Pyramimonas sp.	Chlorophyceae	oboval	10.2	1.73	110.1
Platymonas subcordiformis	Chlorophyceae	oval	10.1	2.59	122.8

	$1+\varepsilon$	Δn (510.6)	n' (440.7)	Q_b	Q_{bb}	b_{bp}/b_p (%)
Prymnesium patelliferum	1.071	0.001	0.0025	1.62	0.006	0.39
Phaeocystis sp.	1.047	0.005	0.0109	2.12	0.007	0.31
Amphidinium sp.	1.037	0.002	0.0048	1.68	0.003	0.17
Chattonella marina	1.046	0.001	0.0036	1.64	0.011	0.69
Microcystis aeruginosa	1.036	0.001	0.0028	2.26	0.020	0.91
Nitzschia closterium	1.038	0.001	0.0038	1.77	0.007	0.38
Thalassirosira weissflogii	1.067	0.001	0.0022	1.81	0.016	0.89
Thalassirosira pseudonana	1.038	0.002	0.0045	1.98	0.007	0.35
Biddulphiales sp.	1.079	0.002	0.0053	1.75	0.010	0.42
Chaetoceros sp.	1.030	0.001	0.0036	1.55	0.008	0.48
Dunaliella tertiolecta	1.053	0.003	0.0049	1.53	0.015	0.97
Tetraselmis levis	1.068	0.002	0.0031	1.53	0.009	0.56
Chlorella sp.	1.077	0.004	0.0075	1.85	0.014	0.74
Pyramimonas sp.	1.052	0.002	0.0028	1.42	0.011	0.75
Platymonas subcordiformis	1.052	0.003	0.0046	1.86	0.013	0.70

ESD is the equivalent spherical diameter from Coulter counter measurements. ESD for spine-forming species includes the spines. Most species are unicellular except for *Chaetoceros* sp., which has chain links.
Optical data are shown at 510 nm.

recorded when stable absorption and attenuation readings were obtained. During each experiment, the container was covered with an opaque black cloth in order to prevent extraneous light from entering the container.

We performed serial dilution tests with each culture to check for linearity of response over five or six concentrations. At the beginning of the experiments for each species, the container was filled with 25 L of 0.45 μm-filtered seawater for marine algae or distilled water for freshwater algae. First, the steady clean-water baseline for each instrument was established, which would be expected to represent the possible effects of the container or filtered media. Next, 30–300 mL samples of culture were added into the container, and the measurements were taken after the algal suspension was thoroughly mixed. Sequential additions of culture were conducted in this fashion until the entire culture had been added. We performed linear regression of the backscattering coefficient and cell density for each culture and found good linearity of response over the range of algal densities tested.

The absorption and attenuation measurements obtained using the acs meter were processed using the software provided with the instrument. Temperature and salinity corrections were performed using contemporaneously recorded CT data (JFE ALEC Inc. ACW-CAR) [26]. The scattering corrections were performed using the baseline method. The backscattering measurements obtained using the BB9 (at 412, 440, 488, 510, 532, 595, 660, 676, and 715 nm) were also processed according to the document provided by the manufacturer. The attenuation corrections were made using the contemporaneously recorded

#161249 - $15.00 USD Received 11 Jan 2012; revised 18 Apr 2012; accepted 19 Apr 2012; published 1 May 2012

beam attenuation and absorption (i.e., acs) data. The value χ_p = 1.1 was used to convert the particulate volume scattering function to the particulate backscattering coefficient [27]. To account for the effect of the container and filtered media, the clean-water baselines were subtracted from the absorption, attenuation, and backscattering coefficients for each cultured suspension. We also had to interpolate some values of the acs scattering estimation in order to match wavelengths for the backscattering ratio calculation.

2.3 Ancillary measurements

The cell size distribution and cell density of the cultures were determined using a Multisizer III Coulter Counter (Beckman Inc.), which provided a reliable size range from 2 to 60 μm in equivalent spherical diameter (ESD). The filtered media counts from the cultures had a negligible effect on the algal cell size distribution and density, so the blank value of the filtered media was not removed from the measurements. The average of three measurements was used to characterize the algal cell size distribution and density.

The POC concentration was obtained using a method described in the JGOFS protocol [28]. The algal suspension was filtered through pre-combusted 25 mm Whatman GF/F filters (450 °C for 5 h) under low vacuum. Following filtration, filters wrapped in aluminum-foil paper were dried at 55 °C and stored in liquid nitrogen until carbon analysis. The determination of POC was made following a standard CHN analysis involving high temperature combustion of sample filters. A CEC 440HA Elemental Analyzer was used. Prior to combustion, 0.25 mL of 10% HCl was applied to each filter to remove inorganic carbon, and the acid-treated filters were re-dried at 55 °C. The final POC concentration values were calculated by subtracting the blank values and then dividing by the measured volume of filtered suspension.

High-performance liquid chromatography (HPLC) was used for pigment analysis using the method developed by Vidussi et al. [29]. Water sample were filtered through 25 mm Whatman GF/F filters. Pigment extraction was performed in 3 ml of methanol. Prior to injection, 500 μl of extract were mixed with 250 μl of 1M ammonium acetate. The extract then was injected through a 200 μl loop into the HPLC system, which was equipped with a 3 μm Hypersil® MOS, 10 cm, 4.6 mm (ID) C8 column (Shandon).

2.4 Optical cross-sections and optical mean efficiency factors

The backscattering cross-section by the population of phytoplankton cells, σ_{bb} (m^2 $cell^{-1}$), was calculated from the backscattering coefficient b_{bp} (m^{-1}) and the algal cell density N/V (cells ml^{-1}) as follows:

$$\sigma_{bb}(\lambda) = \frac{b_{bp}(\lambda)}{N/V} \tag{1}$$

The mean efficiency factors for backscattering $\overline{Q_{bb}}$ (dimensionless) were calculated from the backscattering coefficient b_{bp} (m^{-1}) and the algal cell size distribution as follows:

$$\overline{Q_{bb}}(\lambda) = b_b(\lambda) \times [\frac{\pi}{4} \int_{D\min}^{D\max} F(D) D^2 d(D)]^{-1} \tag{2}$$

where $F(D)d(D)$ is the number of cells per unit volume in the diameter interval $D \pm 1/2d(D)$ [5]. Equations similar to Eq. (1) and Eq. (2) link the scattering cross-section $\sigma_b(\lambda)$ and mean efficiency factor of scattering $\overline{Q_b}(\lambda)$ to the scattering coefficient $b_p(\lambda)$.

#161249 - $15.00 USD Received 11 Jan 2012; revised 18 Apr 2012; accepted 19 Apr 2012; published 1 May 2012

2.5 Homogeneous sphere model for estimating the scattering and backscattering coefficients

The homogenous sphere model was built using an integration of published methods, which were introduced in Bricaud and Morel [5] and refined by Stramski et al. [6] and Bernard et al. [7]. Figure 1 presents a schematic outline of the computational methods.

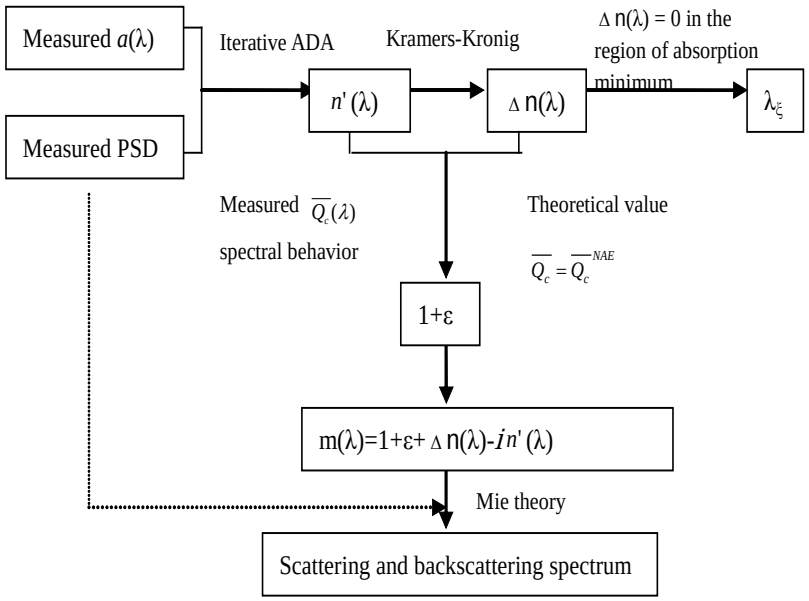

Fig. 1. Schematic representation of the homogenous sphere model used to derive information about the scattering and backscattering spectra from the measured absorption spectrum, particle size distribution, and attenuation spectral behavior.

In this computation, the algal cells are presented as homogenous spheres and are characterized by the complex refractive index relative to that of the surrounding water $m(\lambda) = n(\lambda) - in'(\lambda)$. First, the imaginary part of the refractive index $n'(\lambda)$ is determined using the iterative anomalous diffraction approximation (ADA) procedure of Bricaud and Morel [5], which uses the measured absorption spectrum and particle size distribution (PSD). Next, the real part of the refractive index $n(\lambda)$ is divided into two parts: the central value $1+\varepsilon$ and the spectral variations $\Delta n(\lambda)$. The variation $\Delta n(\lambda)$ is deduced from $n'(\lambda)$ according to the Kramers-Kronig relationship. In $\Delta n(\lambda)$ spectra, there are several cases of wavelength λ where $\Delta n = 0$. In this study, the single wavelength was used where $n'(\lambda)$ is minimum. This wavelength is denoted as λ_ε. At this wavelength λ_ε, the theoretical value of $\overline{Q_c}(\lambda_\varepsilon)$ predicted from Mie theory is iteratively forced to equal the theoretical value of $\overline{Q_c}^{NAE}(\lambda_\varepsilon)$, where $\overline{Q_c}$ is the mean efficiency factor for attenuation and $\overline{Q_c}^{NAE}$ represents the $\overline{Q_c}$ value for the non-absorbing equivalent population with $n'(\lambda_\varepsilon) = 0$. The varying parameter in this procedure is the central value $1+\varepsilon$. The derived results of $1+\varepsilon$ may converge at several different values. To avoid possible multiple solutions, the final choice of $1+\varepsilon$ would be based on a comparison of the spectral attenuation pattern predicted by Mie theory using the selected $1+\varepsilon$ with the experimental pattern. Finally, with the best value of $1+\varepsilon$, the complex refractive index $m(\lambda) = n(\lambda) - in'(\lambda)$ is built, and the scattering and backscattering spectra can be estimated based on Mie theory for each species using the measured PSD.

#161249 - $15.00 USD Received 11 Jan 2012; revised 18 Apr 2012; accepted 19 Apr 2012; published 1 May 2012

2.6 Uncertainties in optical parameters

We estimated the standard deviations of the absorption, attenuation, and backscattering coefficients for all cultures and converted the data to the coefficient of variation (CV). We found that for the 15 species cultured, the absorption measurements had an average (across all wavelengths) CV of 0.2–2.7% and the attenuation measurements had an average CV of 0.2–1.4%. By propagation of error, the uncertainty in the scattering coefficient ranged between 0.2% and 1.4%. The backscattering measurement had an average CV of 1–13%. When combined with the uncertainty of 5.1–13.1% in χ_p at 120 ° depending on the measurement wavelength [24], we estimated the average CV of the backscattering coefficient to be 12–24%. We estimated the uncertainty in the backscattering ratio to be 11–23%. We estimated the uncertainty in particle density and equivalent size diameter to be around 2.4% and 1%, respectively. We estimated the maximum CV in the scattering and backscattering cross-section as 5% and 21%. We estimated the maximum CV in the scattering and backscattering efficiency factors as 8.5% and 18.6%. Two kinds of scattering corrections for the acs data were performed for comparison: (1) baseline correction assuming an absorption coefficient $a(741.5) = 0\ \mathrm{m}^{-1}$, and (2) proportional scattering correction [30]. The results revealed some differences in the magnitude of the retrieved absorption and scattering coefficients between the two correction methods. Such differences varied with the wavelength, and the difference was particularly significant in the green wavebands. For the 15 phytoplankton species tested, the absorption coefficients using different scattering corrections had an average relative deviation of 20%, and accordingly the scattering coefficients had an average relative deviation of 1%. These deviations in absorption coefficients using different scattering corrections would result in an average relative deviation of about 3% and 7% for the estimating scattering and backscattering coefficient using the homogenous sphere model.

3. Results

3.1 Spectral scattering coefficients

The spectral variations in light scattering for the 15 phytoplankton species tested are shown in Fig. 2, where $Q_b(\lambda)$ is the mean efficiency factor for scattering as defined in Eq. (2). Relevant information about these cultures is presented in Table 1. The $Q_b(\lambda)$ values display wide variations from one species to another, ranging between 1.55 and 2.44 at 532 nm. These results are within the range of values (0.28–2.93) reported in the published literature for algal cultures [5,8,9,31,32].

The spectral shape of $Q_b(\lambda)$ exhibits large inter- and intraspecific variability, which is mainly attributed to the variations in size (D) and real refractive index (n) of algal cells [5,31,33]. Theoretical predictions have shown that the value of Q_b is the oscillating function of the parameter $\rho = 2\pi(n-1)D/\lambda$ for algal cultures polydispersed in size (see Fig. 7 of [31]). For example, for *Thalassirosira pesudonana* and *Nitzschia closterium* with $\rho < 3$, the Q_b values tend to decrease with increasing wavelength, as predicted by theory for low ρ values; for the five species of Chlorophyceae, the Q_b values increase slightly with wavelength when the ρ value is generally between 4 and 8. The depressing effect of absorption on spectral $Q_b(\lambda)$ is obvious, such as in the neighborhood of the Chl a absorption band (around 440 nm and 675 nm) and of the chlorophyll b (Chl b) absorption band (around 480 nm), especially for Chlorophyceae [8,31]. Morel and Bricaud [34] provided a detailed theoretical explanation for these behaviors of Q_b in the vicinity of absorption bands.

#161249 - $15.00 USD Received 11 Jan 2012; revised 18 Apr 2012; accepted 19 Apr 2012; published 1 May 2012

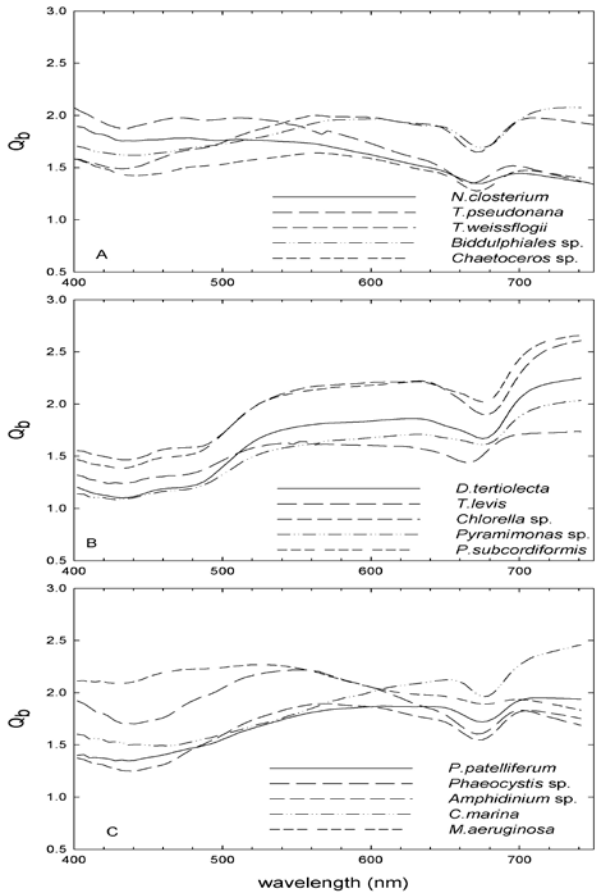

Fig. 2. Scattering efficiency factors Q_b for (A) diatom species, (B) Chlorophyceae species, and (C) other species.

3.2 Spectral backscattering coefficients and backscattering ratios

Figure 3 shows the variability in mean backscattering efficiency factors Q_{bb} for all 15 species tested. The magnitude of Q_{bb} varies strongly from one species to another. For instance, $Q_{bb}(510)$ varies by a factor of nearly 10 and ranges from 0.003 to 0.020. These variations are consistent with the range reported in Vaillancourt et al. [23] and Whitmire et al. [24] measured by HS-6, whereas our measurements are slightly higher than the values (0.000013–0.005 around 550 nm) reported in literature obtained using a spectrometric method [9,30].

The spectral shape of $Q_{bb}(\lambda)$ for these cultures shows distinct features within and between groups. For some species, such as *T. weissflogii*, *T. pseudonana*, and the five species of Chlorophyceae, $Q_{bb}(\lambda)$ shows a peak at ~532 nm. For other species, such as *M. aeruginosa*, *Chaetoceros* sp., *N. closterium*, and *P. patelliferum*, $Q_{bb}(\lambda)$ is essentially spectrally neutral or generally tends to decrease from the blue to the red waveband. The enhanced backscattering peak at 676 nm is obvious for all cultures due to the fluorescence emission superimposed on the backscattering light [9,24,35].

The backscattering ratio $\overline{b_b}$ for these cultures (Fig. 4) ranges from 0.18% to 1.1% at 440 nm, with a medium value of 0.54%. This range was on the low side but basically was within the range (0.35–2.9% at 440 nm) measured using HS-6 [24]. Although there is some spectral

#161249 - $15.00 USD Received 11 Jan 2012; revised 18 Apr 2012; accepted 19 Apr 2012; published 1 May 2012

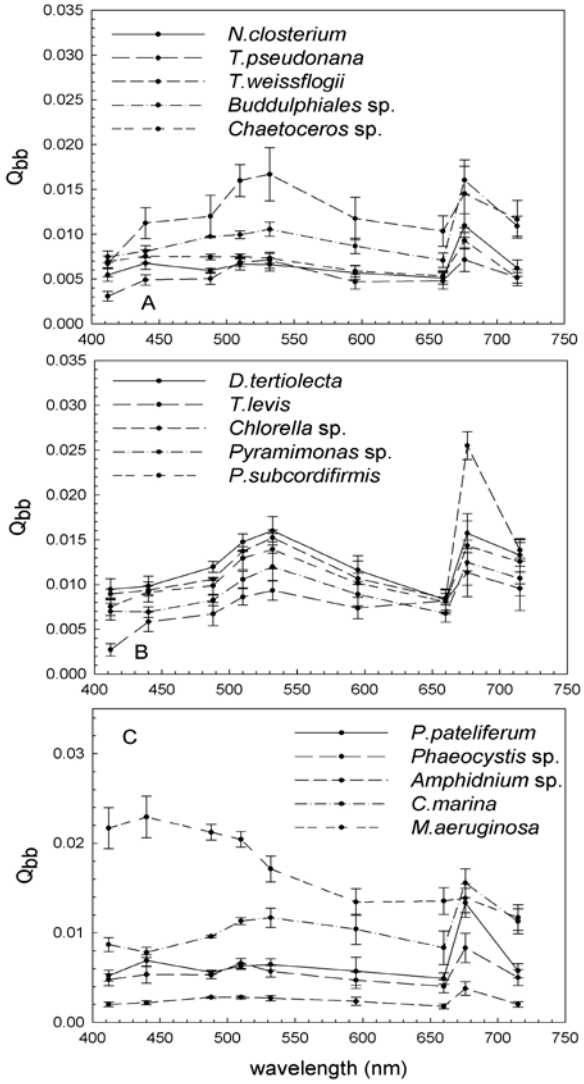

Fig. 3. Backscattering efficiency factors Q_{bb} at nine wavelengths for (A) diatom species, (B) Chlorophyceae species, and (C) other species. Error bars represent one standard deviation of the mean of data.

variability, the differences in backscattering ratios between wavelengths for most species ranges from 11~25%, which is mostly within our measurement deviation of 11~23% for the backscattering ratio. The spectral variability in backscattering ratios for *D. tertiolecta* and *M. aeruginosa* (around 22%) was relatively higher than the measurement deviation of 14% for the backscattering ratio.

3.3 Factors that influence the variability in scattering and backscattering

Variations in cell size are naturally expected to have a major effect on the scattering and backscattering properties of algal cultures. In Fig. 5, the scattering cross-section $\sigma_b(510.6)$ and backscattering cross-section $\sigma_{bb}(510)$ as defined in Eq. (1) are plotted against the ESD

#161249 - $15.00 USD Received 11 Jan 2012; revised 18 Apr 2012; accepted 19 Apr 2012; published 1 May 2012

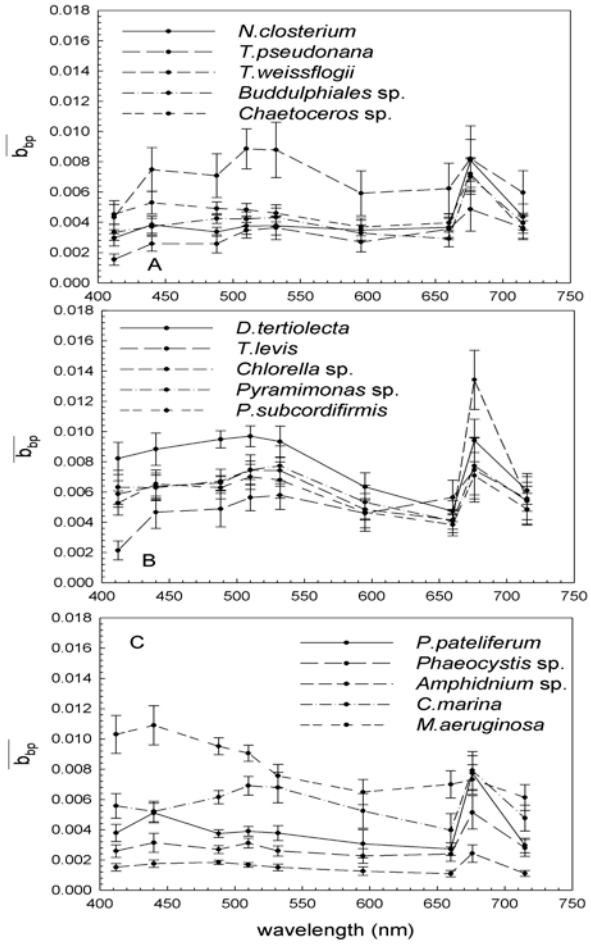

Fig. 4. Backscattering ratio $\overline{b_{bp}}$ at nine wavelengths for (A) diatom species, (B) Chlorophyceae species, and (C) other species. Error bars represent one standard deviation of the mean of data.

(μm) at peak cell density. Nonlinear regression analysis indicates that both $\sigma_b(510.6)$ and $\sigma_{bb}(510)$ are well related to ESD following the power law functions:

$$\sigma_b(510.6) = 3\times10^{-12} ESD^{1.72} \qquad (R^2 = 0.94) \tag{3}$$

$$\sigma_{bb}(510) = 4\times10^{-15} ESD^{2.41} \qquad (R^2 = 0.81) \tag{4}$$

Similar power law relationships were reported in Vaillancourt et al. [23] and Whitmire et al. [24]. For a given cell size, our backscattering cross-section values compared well with those reported by Vaillancourt et al. [23], whereas our data and Vaillancourt's data are on average lower than those reported in Whitmire et al. [24]. These differences may be largely due to the different conversion coefficient χ_p used to convert the $\beta_p(141^\circ)$ to b_b, which was set at ~1.2 in Whitmire et al. [24] but at 0.82 in Vaillancourt et al. [23].

The variation in cellular POC content (Carbon, carbon content per cell, pg cell^{-1}) also has an important effect on the scattering and backscattering cross-section of algal cultures. The trend shown in Fig. 6 indicates that the values of $\sigma_b(510.6)$ and $\sigma_{bb}(510)$ increase proportionally as carbon increases following these equations:

#161249 - $15.00 USD Received 11 Jan 2012; revised 18 Apr 2012; accepted 19 Apr 2012; published 1 May 2012

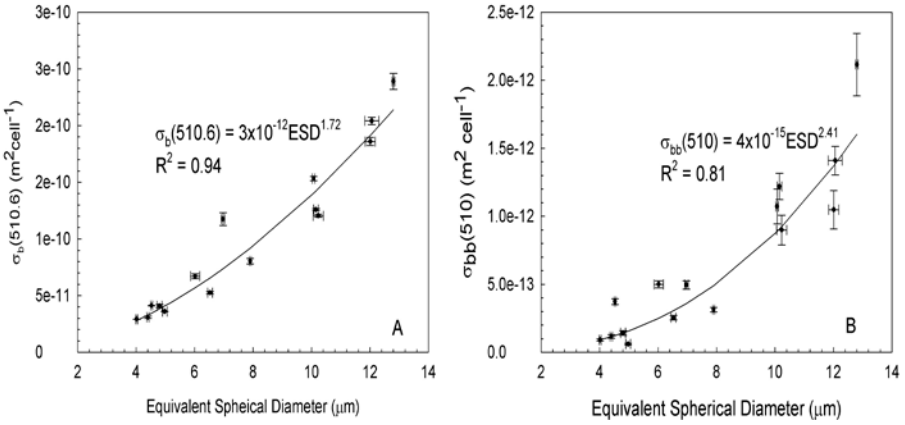

Fig. 5. (A) The scattering cross-section $\sigma_b(510.6)$ versus the equivalent spherical diameter for all cultures; and (B) the backscattering cross-section $\sigma_{bb}(510)$ versus the equivalent spherical diameter for 15 species. Error bars represent one standard deviation of the mean of data.

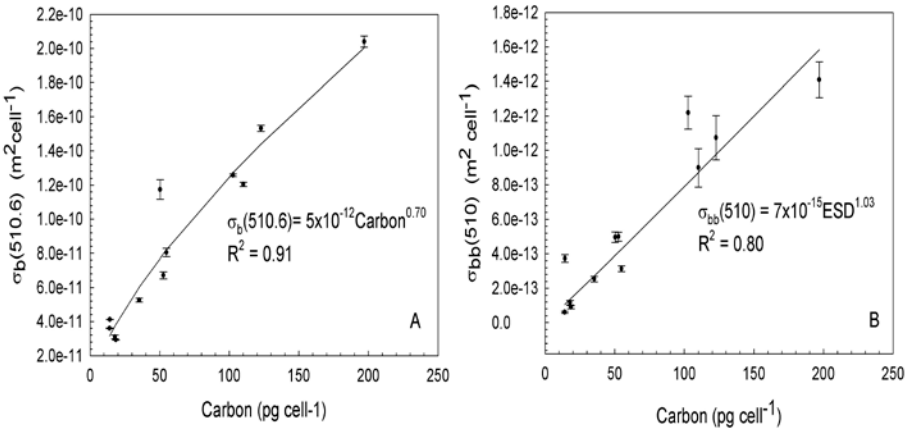

Fig. 6. (A) The scattering cross-section $\sigma_b(510.6)$ versus cellular POC content; and (B) the backscattering cross-section $\sigma_{bb}(510)$ versus cellular POC content. Error bars represent one standard deviation of the mean of data.

$$\sigma_b(510.6) = 5\times10^{-12} Carbon^{0.699} \qquad (R^2 = 0.91) \tag{5}$$

$$\sigma_{bb}(510) = 7\times10^{-15} Carbon^{1.026} \qquad (R^2 = 0.80) \tag{6}$$

Vaillancourt et al. [23] reported a similar relationship. It may be partly due to a close correlation between cellular POC content and cell size ($R^2 = 0.92$). This relationship provides evidence that in situ POC concentration can be derived from scattering measurements [36].

A weak relationship exists between scattering and backscattering cross-section and intracellular POC concentration (*POCi* , carbon content per cell volume, kg m^{-3}), which is interpreted as a proxy of the real refractive index of cells [37]. This probably reflects the intraspecies and interspecies variability in the relationship between *POCi* and the real refractive index for algal cultures.

No significant relationship is found between Chl a per cell and either scattering or backscattering cross-section. Similar conclusions were reached in previous studies of algal

#161249 - $15.00 USD Received 11 Jan 2012; revised 18 Apr 2012; accepted 19 Apr 2012; published 1 May 2012

cultures [23, 24]. In this study, the ratio $b_p(510.6)$: Chl a ranges from 0.042 to 0.523 $m^2 mg^{-1}$, and $b_{bp}(510)$:Chl a ranges from 0.0002 to 0.0036 $m^2 mg^{-1}$.

4. Discussion

4.1 Variability in the spectral backscattering efficiency

In this study, backscattering measurements were made using a BB9 meter at nine wavelengths, which is three more wavelengths than used in Whitmire et al. [24] using a HS-6 meter, and twice as many as in Vaillancourt et al. [23] where only four of the six HS-6 wavelengths were reported. Using this approach, we obtained the backscattering signals at 412 nm and 715 nm. The measurements at 412 nm helped to evaluate the absorption effects on the backscattering spectral pattern, as scattering theory predicts that the chlorophyll absorption at 440 nm has a depressive effect on backscattering signals. From our measurements, we did not observe the significant depressive effect of absorption at 440nm on the backscattering signals. The backscattering efficiencies at 412 for most species are close to the values at 440nm. Several of the backscattering spectra even showed a decreasing trend from 440 nm to 412 nm. It is possible that more usable wavelengths measurements in the backscattering meter would provide sufficient information to examine the detailed backscattering spectral feature within the absorption bands. Our measurements also included the backscattering signals at 715 nm, which increased for most species if the fluorescence contamination signals at 676 nm were excluded. It is not clear why the backscattering efficiency at 715nm increases for most species. However, the estimated backscattering spectra from the homogenous sphere model in Stramski et al. [13] [as shown in their Fig. 3] showed the increasing backscattering at 715 nm for some species. Our backscattering coefficient estimated by the homogenous sphere model also showed an increase at 715 nm for most species (as shown in our Fig. 8).

We took backscattering measurements at four wavelengths from 500nm to 660 nm (e.g. 510, 532, 595, 660 nm), while Whitmire et al. [24] reported the values at three wavelengths (e.g. 532, 555, 620 nm) and Vaillancourt et al. [23] reported the values at only two wavelengths (510 and 620 nm), These wavelengths were used to examine trends in the backscattering spectra of phytoplankton over a range of wavelengths. We found that the backscattering spectra did not follow a generalized decreasing trend from 412 nm to 660 nm for most species, which is inconsistent with the observation in Vaillancourt et al. [23] using only two wavelengths. Several of our backscattering spectra showed a peak at ~532 nm and a decrease at the adjacent 595 nm. The backscattering measurements in Whitmire et al. [24] also observed the increasing signals with a peak around 532 nm or 555 nm relative to the values at adjacent wavelengths for some species. Stramski et al. [13],who presented the backscattering results derived from models for 18 species, also showed that backscattering signals might exhibit a peak that ranged between 510 nm and 590 nm for different species [as shown in their Fig. 3]. Such measurements and theoretical results indicated that backscattering spectra might have significant spectral variability across 500~600 nm. Therefore, the backscattering measurements taken at more wavelengths might provide a more realistic description of spectral behaviors. Backscattering values measured at more wavelengths, especially around absorption wavebands, might also help to investigate the relationship between backscattering spectral features and phytoplankton properties.

4.2 Variability in the backscattering efficiency and backscattering ratio between cultures

In this study, backscattering efficiencies for the diatoms were highly variable, ranging from 0.003 to 0.016 (Table 1). Both the backscattering efficiency and backscattering ratio appear to be the linear functions of size for these diatoms (R^2 = 0.968 and R^2 = 0.954, respectively). The larger diatoms generally seemed to have higher backscattering efficiencies and larger

#161249 - $15.00 USD Received 11 Jan 2012; revised 18 Apr 2012; accepted 19 Apr 2012; published 1 May 2012

backscattering ratios than the smaller diatoms. For two species with similar cell shape and similar internal structure, larger *T. weissflogii* had much higher Q_{bb} and higher $\overline{b_b}$ values than those for smaller *T. pseudonana*. These results disagree with the simplistic scattering model interpretation for homogenous particles, because all else being equal, a larger homogenous particle has a lower backscattering ratio than a smaller homogenous particle. Whitmire et al. [24] also observed a positive relationship between diatom size and backscattering ratio, which they attributed to the influence of detrital and bacterial contamination, the effect of complex internal structure, or the distorted interpretation of the simplistic model. Non-algal particles, such as detritus and bacteria, were also unavoidable components of our cultures. We speculate that larger cells might have much more subtle refractile granules, such as assimilation product starch granules, oil spots, etc. Since these subtle granules have small size and high refractive index, they could increase the backscattering signals significantly. Thus, if the cell shape and internal structure of two species are similar, a larger cell containing more subtle refractile granules might have a higher backscattering ratio.

Compared to the backscattering efficiencies of diatoms, the members of the Chlorophyceae generally had higher backscattering efficiencies (0.0086 to 0.0148, Table 1). This may be due to the large cell size of these species. For example, *D. tertiolecta*, *T. levis*, *Pyramimonas* sp., and *P. subcordiformis* all are 10–12 μm in diameter, whereas four species of diatom (except *T. weissflogii*) are <7 μm in size. In addition to large cell size, the Chlorophyceae in our cultures had relatively high real refractive indices, which may increase their high backscattering efficiencies. The high real refractive index for our chlorophytes might be mainly contributed by a large cup-shaped chromatophore and the pyrenoids in cells. The large cup-shaped chromatophore can occupy relative large cell volume, about one-half of the cells especially in *Chlorella* sp. [38].The chromatophore is rich in pigments, such as the β-carotenoid in *D.tertiolecta* could account for 10% of dry weight [38]. The chromatophore and pyrenoids are primarily composed of high density substances (e.g. proteins, lipids and pigments), which can have a refractive index as high as 1.13–1.19 relative to water [39]. Therefore, we speculate that such substances in our chlorophytes would significantly increase the backscattering properties by increasing the real refractive index of the algal cells.

The backscattering efficiency for chlorophytes did not seem to relate to their size. The differences in concentration of the intracellular dispersed substance among species might be another important factor dominating the variability of backscattering efficiency. The intracellular carbon concentration POC_i is an indicator of the characterization of concentration of the dispersed substance. If the algal cells among different species have similar proportions of primary elements (e.g. carbon, hydrogen, oxygen and nitrogen), the POC_i can be assumed to be related to the density of algal cells, which would be related to the refractive increment [37]. Among our chlorophytes, the small *Chlorella* sp. has a twice as high POC_i (466 kg m^{-3}) as *D. tertiolecta*, *Pyramimonas* sp.and *P. subcordiformis*(around 200 kg m^{-3}).We speculate that the high POC_i of *Chlorella* sp. is related to the high real refractive index, which would contribute to the backscattering efficiency as much as the other three species. Besides, the large *T. levis* had a low backscattering efficiency. We lacked the measurements of POC_i for *T. levis*. While the measurements from Liu [40] showed that the ratio of carbon and nitrogen for *T. levis* (C:N = 4:1) was significantly lower than the ratio(C:N = 8:1) for *D. tertiolecta*. Although the C:N of the same species cultured might be variable under different environment [41], such large difference of C:N between *T. levis* and *D. tertiolecta* would indicate the difference in cell compositions between them. This speculation might imply that the differences in cell component between species may be responsible for the magnitude in backscattering efficiency.

The only dinoflagellate examined in this study, *Amphidinium* sp., exhibited a relatively low backscattering efficiency of 0.003 at 510 nm in our cultures. This is inconsistent with the fact that dinoflagellates had the highest backscattering efficiency among the phytoplankton

#161249 - $15.00 USD Received 11 Jan 2012; revised 18 Apr 2012; accepted 19 Apr 2012; published 1 May 2012

studied both in Vaillancourt et al. [23] and Whitmire et al. [24]. These authors speculated that the high backscattering efficiency might be due to the relatively high intracellular carbon concentration and the presence of some unique internal structures and very unusual chromosome morphology of dinoflagellates. However, *Amphidinium* sp. does not have a high carbon contentration, and it is also small in size. Vaillancourt et al. [23] showed that the backscattering efficiency factor would decrease as cell size and intracellular carbon concentration decrease. Thus, it is possible that the relatively low carbon concentration and small size could explain the low backscattering efficiencies we observed for *Amphidinium* sp.

The sole cyanophyte examined in this study, *M. aeruginosa*, exhibited the relatively high backscattering efficiency of 0.020 and backscattering ratio of 0.91% at 510 nm. The gas-filled vesicles in *M. aeruginosa* may greatly contribute to increased backscattering [21].

The spectral shape of the sole Raphidophyceae *C. marina* strongly resembled those for five species of chlorophytes. We hypothesize that the similar spectral pattern might be attributed to their similarity in cell shape and cellular structure. First, both *C. marina* and the chlorophytes are oval or spherical in shape. In addition to their similarity in cell shapes, all of them have no cell wall or thin cell wall, which might imply that their internal structures play a large role in backscattering. Our chlorophytes have a large cup-shape chloroplast. *C. marina* has numerous radially arranged chloroplasts [42]. Since such arrangements of chloroplasts in *C. marina* are compact, we speculate the backscattering characteristics of these chloroplasts might be equivalent to backscattering characteristics of one large chloroplast in our chlorophytes. Moreover, The main pigment components in Raphidophyceae are similar to those in our chlorophytes [42], which might also contribute to the similar spectral behaviors of backscattering among them.

4.3 Comparisons of measured vs. modeled values of scattering and backscattering

We compared the scattering and backscattering coefficients obtained from our measurements with the values predicted by the homogenous sphere model. The main features of the measured b_p spectra for all species were fairly well reproduced by the model, as shown in Fig. 7. The depressive effects of the absorption bands of Chl a and Chl b on b_p spectra were also reproduced by the model. Both the magnitude and spectral shape of the modeled b_p were generally comparable with the measurements. The mean relative deviation for all species ranged from 5% to 39%, with a mean value of 17%. The minimum deviation was observed for *Chlorella* sp., which may be largely due to the similarity between the actual morphology of the cell and the assumption of the sphericity and homogeneity of the model. For species with a relatively large deviation, the spectral slopes of the modeled b_p often were steeper than those of the measured results. The non-spherical shape and/or heterogeneities of cells explain these divergences. Some studies have shown that particles with a layered internal structure [8,16,43] or a randomly oriented non-spherical shape [18] could result in a smoother slope for the scattering spectra than for those represented as homogenous spheres. In our study, the species tested were mostly ovoid and cylinder, and large heterogeneities were also introduced by the highly refractive cell walls for diatom or the presence of peripheral chloroplasts for other species. It is difficult to know if the cellular morphology or the cellular structure causes the measurements to deviate from theory using the homogenous sphere model. The layered sphere model or an non-spherical model might provide more information about the effect of cellular morphology and complex structure on backscattering properties [16,18,43].

In this study, the modeled backscattering spectra were scaled to coincide with the measured data at 510 nm, as shown in Fig. 8. The ratio of measured to theoretical values at 510 nm is denoted *Ratio*.

#161249 - $15.00 USD Received 11 Jan 2012; revised 18 Apr 2012; accepted 19 Apr 2012; published 1 May 2012

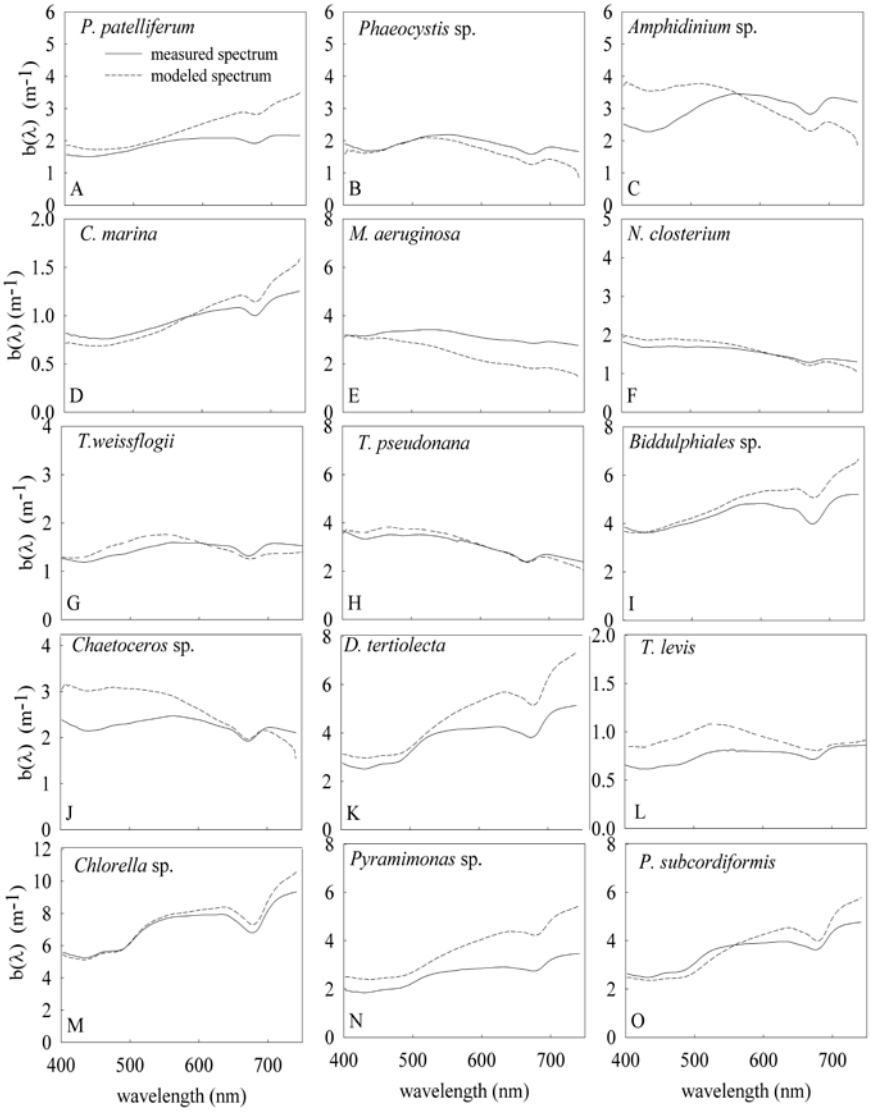

Fig. 7. Comparison between the measured spectral scattering coefficient (solid lines) and the modeled spectrum (dotted lines) from the homogeneous spherical model for the 15 phytoplankton species tested.

The homogeneous sphere model severely underestimated the backscattering coefficient by 1.4–48.6 folds at 510 nm. The quantitative results provide further evidence for the inadequacy of the homogenous spherical model for estimating the backscattering of algal cultures [23,44]. Calavano et al. [18] reported that backscattering for spheroid particles tends to be several-fold higher than that for spherical particles. In our study, the *Ratio* seemed to be strongly dependent on cell shape. A relatively small deviation (*Ratio* = 2) was observed for spherical species, such as *Chlorella* sp., whereas the *Ratio* ranged from 2 to 16 for ovoid or ellipsoidal species. Moreover, the *Ratio* reached 33 for *Chaetoceros* sp. because of the chain link nature of the cells. Cell heterogeneities also had an influence on the *Ratio* . Some researchers have shown that backscattering predicted by a multi-layered sphere can be higher than that by a homogenous sphere [16,43,44]. In particular, the magnitude of backscattering was most

#161249 - $15.00 USD Received 11 Jan 2012; revised 18 Apr 2012; accepted 19 Apr 2012; published 1 May 2012

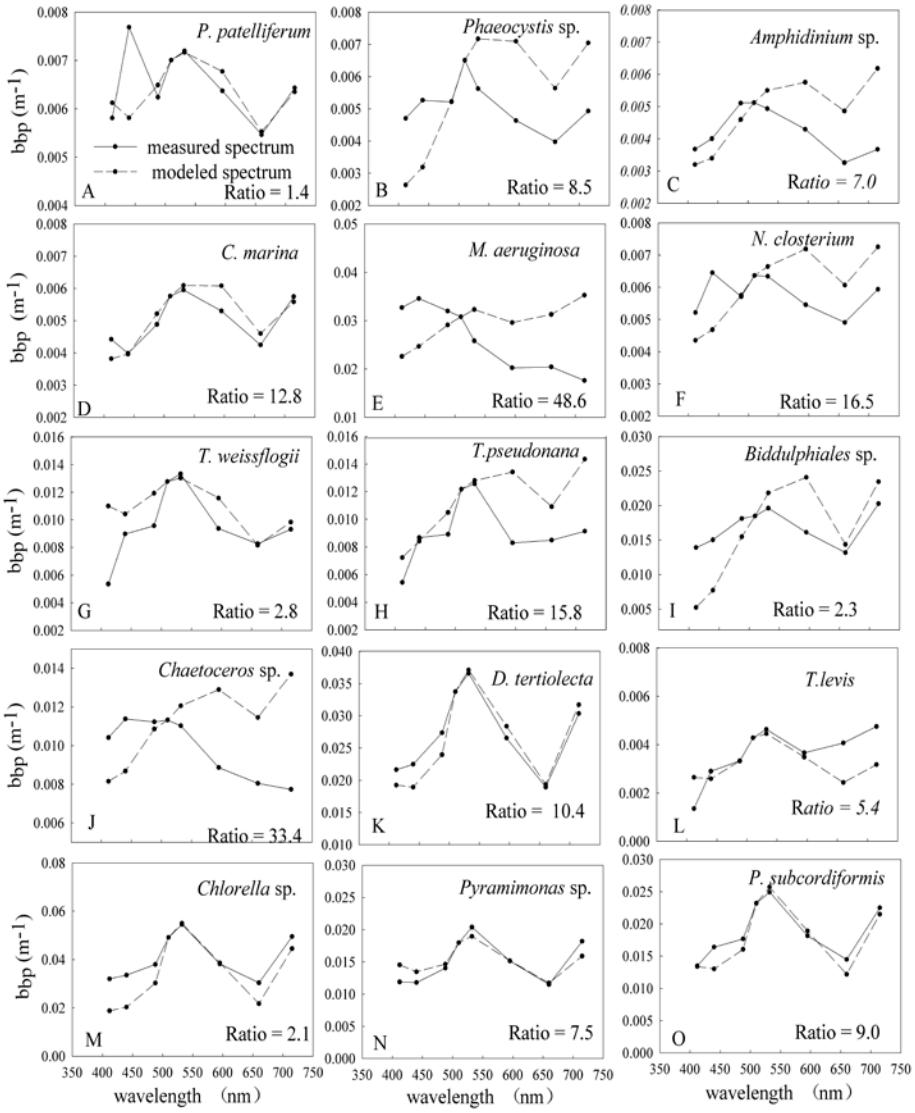

Fig. 8. Comparison between the measured backscattering coefficients at eight wavelengths and the modeled values as computed using the Mie theory for 15 phytoplankton species. The modeled backscattering coefficients were adjusted to the measured values at 510 nm to facilitate comparison of the spectral shapes. The ratios of the measured $b_{bp}(510)$ and the modeled $b_{bp}(510)$ values, denoted *Ratio*, are given for each species.

sensitive to the thickness of cell walls [15]. In this study, *M. aeruginosa* had pronounced gas-filled vacuoles, which would significantly affect the magnitude and spectral pattern of backscattering, and the *Ratio* would reach 48.6. The diatoms had refringent cell walls, and most of the other species had peripheral chloroplasts; these heterogeneities might have contributed to the increased backscattering compared to the predictions made by the homogeneous sphere model.

#161249 - $15.00 USD Received 11 Jan 2012; revised 18 Apr 2012; accepted 19 Apr 2012; published 1 May 2012

5. Conclusion

The spectral scattering and backscattering properties of 15 phytoplankton species were estimated using the acs and BB9 instruments in the laboratory. We also collected samples to measure Chl a concentration, POC content, cell concentration, and the particle size distribution. The objective of the study was to examine the influence of cell size, organic carbon content, shape, and internal structure on variations in scattering properties. In addition, we quantitatively compared the measurements with the scattering and backscattering coefficients predicted by the homogenous sphere model for 15 phytoplankton species.

We observed the variability in the scattering and backscattering spectra of the 15 species studied. The backscattering efficiency at 412 was not always higher than those at 440nm. Several of the backscattering spectra had a peak at ~532 nm, and the backscattering efficiency at 715 nm increased for some species. These observations indicated that there might be significant spectral variability in the backscattering spectra. The backscattering measurements taken at more wavelengths might provide a more realistic description of spectral behavior.

We reconfirmed the strong relationships between backscattering cross-sections and both cell size (ESD) and carbon content. We also found positive correlations between cell size and both backscattering efficiency and backscattering ratio, and these relationships were similar to those reported in Whitmire et al. [24].

A comparison of our measurements with values modeled using the homogenous sphere model showed that the Mie theory for homogenous spheres could provide a good description of scattering coefficients, both in magnitude and in spectral shape, for the 15 species tested. This indicates that cell shape and internal structure might have no significant effect on predicting the scattering properties using Mie theory. However, the comparison for the backscattering spectra showed that the Mie theory for homogenous spheres is not a good method for modeling backscattering of algal species. The model underestimated the backscattering coefficients by 1.4–48.6 folds. External cell shape, such as the chain link structure, and complex internal structures, such as refractive cell walls, peripheral chloroplasts, gas vacuoles, might significantly affect the model's prediction of backscattering behavior. Our results suggest that further studies and a better understanding of spectral backscattering properties of non-spherical and non-homogenous algal species are needed. Research using a layered sphere model or an ellipsoidal model might improve our understanding of how morphology or internal structure influences the backscattering properties of algal species.

Acknowledgments

We thank the Marine Biology Group of the South China Sea institute of Oceanography (SCSIO) for providing the algal species and Wei Xiao for algae cultivation. We thank the team headed by Prof. Xiaoling Chen of the State Key Laboratory of Information Engineering in Surveying, Mapping and Remote Sensing at Wuhan University for providing the acs and BB9 instruments and Liqiong Chen for her help with taking the measurements. We are indebted to all of our associates in the ocean optics group at the SCSIO for their help. We appreciate the thoughtful comments from all reviewers, which helped to greatly improve an earlier version of this manuscript. This study was funded by the National Natural Science Foundation of China (Grant Nos. 40906022, 41076014, U0933005, 40906021) and the Knowledge Innovation Program of the Chinese Academy of Sciences (Grant No. SQ201003).

#161249 - $15.00 USD Received 11 Jan 2012; revised 18 Apr 2012; accepted 19 Apr 2012; published 1 May 2012